

## Comparing Ion Exchange Adsorbents for Nitrogen Recovery from Source-Separated Urine

William A. Tarpeh, Kai M Udert, and Kara L. Nelson

*Environ. Sci. Technol.*, **Just Accepted Manuscript** • DOI: 10.1021/acs.est.6b05816 • Publication Date (Web): 18 Jan 2017

Downloaded from <http://pubs.acs.org> on February 2, 2017

### Just Accepted

“Just Accepted” manuscripts have been peer-reviewed and accepted for publication. They are posted online prior to technical editing, formatting for publication and author proofing. The American Chemical Society provides “Just Accepted” as a free service to the research community to expedite the dissemination of scientific material as soon as possible after acceptance. “Just Accepted” manuscripts appear in full in PDF format accompanied by an HTML abstract. “Just Accepted” manuscripts have been fully peer reviewed, but should not be considered the official version of record. They are accessible to all readers and citable by the Digital Object Identifier (DOI®). “Just Accepted” is an optional service offered to authors. Therefore, the “Just Accepted” Web site may not include all articles that will be published in the journal. After a manuscript is technically edited and formatted, it will be removed from the “Just Accepted” Web site and published as an ASAP article. Note that technical editing may introduce minor changes to the manuscript text and/or graphics which could affect content, and all legal disclaimers and ethical guidelines that apply to the journal pertain. ACS cannot be held responsible for errors or consequences arising from the use of information contained in these “Just Accepted” manuscripts.

# Comparing ion exchange adsorbents for nitrogen recovery from source-separated urine

William A. Tarpeh<sup>†#</sup>, Kai M. Udert<sup>‡</sup>, Kara L. Nelson<sup>†##</sup>

<sup>†</sup>Department of Civil and Environmental Engineering, University of California, Berkeley, CA 94720, United States

<sup>#</sup>Engineering Research Center for Re-inventing the Nation's Urban Water Infrastructure (ReNUWIt), United States

<sup>‡</sup>Eawag, Swiss Federal Institute of Aquatic Science and Technology, 8600 Dübendorf, Switzerland

Submitted to:

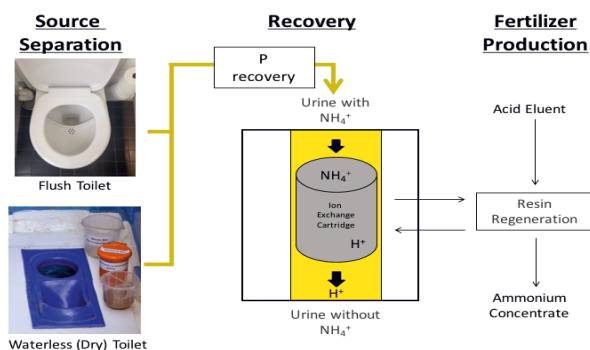
*Environmental Science & Technology*

November 2016

\*Corresponding author: [karanelson@berkeley.edu](mailto:karanelson@berkeley.edu)

## 46 TOC

47



48

49

## 50 ABSTRACT

51 Separate collection of urine, which is only 1% of wastewater volume but contains the majority of  
 52 nitrogen humans excrete, can potentially reduce the costs and energy input of wastewater  
 53 treatment and facilitate recovery of nitrogen for beneficial use. Ion exchange was investigated for  
 54 recovery of nitrogen as ammonium from urine for use as a fertilizer or disinfectant. Cation  
 55 adsorption curves for four adsorbents (clinoptilolite, biochar, Dowex 50, and Dowex Mac 3)  
 56 were compared in pure salt solutions, synthetic urine, and real stored urine. Competition from  
 57 sodium and potassium present in synthetic and real urine did not significantly decrease  
 58 ammonium adsorption for any of the adsorbents. Dowex 50 and Dowex Mac 3 showed nearly  
 59 100% regeneration efficiencies. Estimated ion exchange reactor volumes to capture the nitrogen  
 60 for one week from a four-person household were lowest for Dowex Mac 3 (5 L) and highest for  
 61 biochar (19 L). Although Dowex Mac 3 had the highest adsorption capacity, material costs (\$/g  
 62 N removed) were lower for clinoptilolite and biochar because of their substantially lower unit  
 63 cost.

64

## 65 1. INTRODUCTION

66 Source separation, in which urine and feces are separated at the toilet, has recently emerged as a  
67 potential alternative to conventional wastewater management, in which all wastewater is  
68 combined and treated together.<sup>1</sup> Separately collecting and treating distinct waste streams could  
69 allow for more optimal approaches to recover embedded resources,<sup>2</sup> and reduce energy and  
70 financial costs for wastewater treatment.<sup>3,4</sup> Conventional biological treatment removes nitrogen  
71 as dinitrogen gas (N<sub>2</sub>); this process simply reverses energy-intensive fertilizer production via the  
72 Haber-Bosch process, from which most of the wastewater nitrogen was derived.<sup>5</sup> Recovering  
73 reduced nitrogen directly from wastewater closes the loop between fertilizer production and  
74 wastewater treatment more efficiently than using N<sub>2</sub> as an intermediate. Urine has emerged as a  
75 waste stream of increasing interest because it comprises only 1% of wastewater volume but  
76 contains the majority of excreted macronutrients.<sup>1</sup> Furthermore, nitrogen-based fertilizers and  
77 disinfectants could potentially be a revenue source;<sup>6,7</sup> this creation of valuable products  
78 distinguishes recovery from removal.

79  
80 Source separation could potentially be integrated into existing centralized wastewater  
81 infrastructure to reduce nutrient loads on wastewater treatment plants.<sup>8</sup> For example, as San  
82 Francisco and Paris are facing potential large capital investments to remove nitrogen from  
83 wastewater to reduce eutrophication in receiving waters,<sup>9,10</sup> source separation and resource  
84 recovery technologies are being considered.<sup>11</sup> Source separation could also be used to reduce  
85 nitrogen loads from on-site sanitation due to failing septic systems,<sup>4</sup> and in urban areas that lack  
86 formal infrastructure, such as the decentralized approaches being pursued by Sanergy in low-  
87 income, high-density settlements in Nairobi, Kenya<sup>12</sup> and the Valorization of Urine Nutrients

88 (VUNA) project in Durban, South Africa.<sup>13</sup> To inform the choice between source  
89 separation/resource recovery and current wastewater management approaches, technologies that  
90 enable the new paradigm must be further developed and more rigorously characterized.

91  
92 Ion exchange is a promising technology for nitrogen recovery from source-separated urine.  
93 During urine storage, urea is hydrolyzed to ammonium ( $\text{NH}_4^+$ ),<sup>14</sup> which can adsorb onto  
94 materials with negatively charged sites. Although cation exchange has been studied for removing  
95  $\text{NH}_4^+$  from  $\text{NH}_4\text{Cl}$  solutions,<sup>15</sup> drinking water,<sup>16</sup> and landfill leachate<sup>17</sup> at concentrations less than  
96 800 mg N/L, it has only been preliminarily documented for urine treatment, which has  $\text{NH}_4^+$   
97 concentrations of around 5000 mg N/L.<sup>18</sup> Multiple studies have examined sorption of phosphate  
98 and pharmaceuticals from synthetic urine by anion exchange resins.<sup>19,20</sup> Cation exchange  
99 adsorbents could also be used for potassium recovery. Suitable adsorbents can be selected and  
100 combined to remove the resources or pollutants of interest. As a physicochemical process,  
101 sorption may be more stable than biological nitrogen removal. Because the required adsorbent  
102 mass and reactor size are proportional to the mass of compound removed, sorption can be  
103 applied at varying scales. Sorption's selective, stable, and scalable nature make it a promising  
104 option for resource recovery from urine.<sup>21</sup>

105  
106 To our knowledge, this investigation is the first to compare the feasibility of a diverse set of ion  
107 exchange adsorbents for cation recovery from source-separated urine. Four ion exchange  
108 adsorbents were tested: clinoptilolite, biochar, Dowex 50, and Dowex Mac 3. Clinoptilolite is  
109 extremely abundant, naturally-occurring, and has been documented for removing ammonium  
110 from drinking water,<sup>22</sup> wastewater,<sup>22,23</sup> and, preliminarily, source-separated urine.<sup>24</sup> Biochar is

111 already being used as a soil conditioner for nutrient and moisture retention and can be produced  
112 economically from a variety of feedstocks.<sup>25,26</sup> One such feedstock is feces, which could make  
113 possible a scheme in which feces-based biochar is used to recover ammonium from separately  
114 collected urine. Dowex 50 is a standard synthetic cation exchange resin, and Dowex Mac 3 is  
115 another synthetic cation resin with purported ammonium specificity,<sup>27</sup> suggesting it may be  
116 particularly suited to ammonium recovery from source-separated urine.

117  
118 In this study, factors affecting ammonium adsorption were explored in solutions of increasing  
119 complexity: pure salt, synthetic urine, and real urine. Experiments were designed to measure two  
120 major determinants of feasibility: adsorption capacity and regeneration potential. Adsorption  
121 capacity describes how much nitrogen can be captured each sorption cycle per mass of adsorbent  
122 (before regeneration) and can be used to determine minimum reactor size. Regeneration potential  
123 influences adsorbent lifetime, and therefore how much urine the adsorbent can treat before  
124 replacement. The specific objectives of this study were to: (i) characterize adsorption in ideal  
125 solutions with respect to the Langmuir parameters maximum adsorption density,  $q_{\max}$ , and  
126 affinity constant,  $K_{\text{ads}}$ ; (ii) characterize adsorption isotherms in synthetic and real urine, including  
127 the effect of sodium and potassium competition on ammonium adsorption; (iii) determine  
128 adsorption capacity and regeneration efficiency in column experiments; and (iv) estimate  
129 adsorbent costs and reactor volume to preliminarily assess the feasibility of ion exchange for  
130 nitrogen recovery from source-separated urine.

131

## 132 **2. MATERIALS AND METHODS**

### 133 **2.1 Description of Adsorbents**

134 Four adsorbents were examined in this study: clinoptilolite (Multavita, Castle Valley, MT),  
135 biochar (Ithaca Institute, Ayent, Switzerland), Dowex 50 (Alfa Aesar, Ward Hill, MA), and  
136 Dowex Mac 3 (Sigma Aldrich, St. Louis, MO). Clinoptilolite is an aluminosilicate zeolite with  
137 negatively charged sites due to the isomorphic substitution of trivalent aluminum for tetravalent  
138 silicate groups. As the most abundant natural zeolite, it is isolated from naturally occurring  
139 mineral deposits in many countries, including Turkey, South Africa, Australia, China, and the  
140 United States.<sup>22</sup> Biochar is a carbon-rich product made by thermal decomposition of organic  
141 material under limited supply of oxygen and at a temperature greater than 700°C.<sup>28</sup> Within this  
142 definition, biochar varies extensively in form, feedstock, and processing method. The biochar  
143 used in this study was from wood husks (950°C for 2 hours, no pretreatment); similar biochars  
144 have carboxyl functional groups.<sup>26</sup> The adsorption sites of Dowex 50 and Dowex Mac 3 are  
145 sulfonic acid and carboxylic acid moieties, respectively. This difference in functional groups  
146 makes Dowex 50 effective over a wider pH range than Dowex Mac 3.<sup>27,29</sup> Both Dowex resins are  
147 available with protons initially adsorbed to functional sites. Dowex Mac 3 is marketed as an  
148 ammonium-specific cation exchange resin produced from a polyacrylic matrix and added  
149 carboxylate moieties.<sup>27</sup> For further information on adsorbents see Table S1.

150

## 151 **2.2 Solution Types**

152 To examine the factors and mechanisms affecting adsorption in urine, four solutions were used,  
153 ranging from ideal to real: (i) NH<sub>4</sub>Cl without pH adjustment; (ii) NH<sub>4</sub>Cl at pH 9; (iii) synthetic  
154 stored urine (pH ~ 9); and (iv) real stored urine (pH ~ 9). Because NH<sub>4</sub><sup>+</sup> is a weak acid (pK<sub>a</sub>  
155 9.25)<sup>30</sup>, the pH of the 9000 mg N/L NH<sub>4</sub>Cl solution without adjustment was 4.72. For ease of  
156 reference, we call these “pH 4 experiments.” The effect of pH on ammonium adsorption was

157 elucidated by comparison with pH 9  $\text{NH}_4\text{Cl}$ , which is closer to the pH of stored urine and the  
158  $\text{NH}_4^+/\text{NH}_3$   $\text{pK}_a$ . Synthetic stored urine was used to observe the effect of competition on  
159 ammonium adsorption by other cations, such as  $\text{Na}^+$  and  $\text{K}^+$ . We used an existing synthetic urine  
160 recipe based on real urine concentrations (Table S2).<sup>31</sup> Organic acids are the primary organic  
161 constituent of urine;<sup>31</sup> acetic acid is used in synthetic urine to represent organic acids. Finally,  
162 real source-separated urine from NoMix toilets and waterless urinals was used.<sup>7</sup> The real urine  
163 was from the men's collection tank of the Swiss Federal Institute of Aquatic Sciences and  
164 Technology's (Eawag) main building *Forum Chriesbach* (composition in Table S3). Given the  
165 extended storage time, urea was completely hydrolyzed to ammonia/ammonium and magnesium  
166 and calcium concentrations were negligible due to struvite and hydroxyapatite precipitation.<sup>32</sup> In  
167 addition to the four solution types above,  $\text{NaCl}$  and  $\text{KCl}$  solutions were also prepared without pH  
168 adjustment. These results served as inputs for competitive adsorption models to which synthetic  
169 urine results were compared. All experiments were conducted at room temperature ( $23 \pm 2$  °C)  
170 with nanopure water and analytical grade chemicals.

171

### 172 **2.3 Batch Adsorption Experiments**

173 Batch adsorption experiments were conducted by adding 0.015 g adsorbent to 1.5 mL of solution  
174 and continuously mixing for 24 hours to ensure equilibration (based on preliminary  
175 experiments). Samples were then centrifuged at 2000 rpm for five minutes to separate adsorbent  
176 and solution. Aliquots from the initial solution and the supernatant were analyzed for  $\text{NH}_4^+$ ,  $\text{Na}^+$ ,  
177 and  $\text{K}^+$  concentrations via ion chromatography (Metrohm chromatograph, IonPac CS12 column,  
178 30 mM methanesulfonic acid eluent, 1.0 mL/min, 30 °C). A six-cation chloride calibration  
179 standard ( $\text{LiCl}$ ,  $\text{NaCl}$ ,  $\text{NH}_4\text{Cl}$ ,  $\text{KCl}$ ,  $\text{MgCl}_2$ ,  $\text{CaCl}_2$ ) was diluted 100, 50, 20, 10, and 6.25 times to



180 generate a calibration curve. A mass balance was used to calculate the final adsorption density  
181 ( $q_f$ ) at equilibrium according to Equation 1:

$$182 \quad V_L(C_0 - C_f) = W(q_f - q_0) \quad (1)$$

183 where  $V_L$  is solution volume (L),  $C_0$  is initial concentration of adsorbate (mg  $\text{NH}_4^+$ -N,  $\text{Na}^+$ , or  
184  $\text{K}^+$ /L),  $C_f$  is adsorbate concentration at equilibrium (mg  $\text{NH}_4^+$ -N,  $\text{Na}^+$ , or  $\text{K}^+$ /L),  $W$  is adsorbent  
185 mass (g), and  $q_0$  is the initial adsorption density (mg  $\text{NH}_4^+$ -N,  $\text{Na}^+$ , or  $\text{K}^+$ /g adsorbent). To  
186 compare adsorption densities between cation species, molar mass was used to convert adsorption  
187 densities to mmol/g adsorbent.

188  
189 For pH 4 experiments, 16 initial  $\text{NH}_4\text{Cl}$  solutions with ammonia concentrations varying from 25-  
190 9000 mg N/L were prepared without pH adjustment. For pH 9 experiments,  $\text{NH}_4\text{OH}$  was added  
191 to increase pH. For synthetic and real urine experiments, one master solution was made and  
192 diluted to 15 different concentrations to generate adsorption curves. Real urine was filtered (0.47  
193  $\mu\text{m}$ ) to exclude precipitates that might have interfered with adsorption. Although initial pH  
194 differed for each dilution in a given adsorption curve, we refer collectively to each set of  
195 experiments by the pH of the most concentrated initial solution. For example, we refer  
196 collectively to samples prepared from the 9000 mg N/L  $\text{NH}_4\text{Cl}$  at pH 9 as “pH 9 experiments”  
197 although pH was less than 9 for many dilutions.

198

## 199 **2.4 Continuous Adsorption Experiments**

200 Upflow continuous adsorption experiments were performed in PVC columns (2.54-cm diameter,  
201 16-cm length) packed with each adsorbent, sponges to retain media, and pretreated with 1 M  
202 borate buffer. Synthetic urine was pumped through each column at 4.5 mL/min for 6 hours, and

203 samples from the end of the column were collected every 20 minutes and analyzed for  
 204 ammonium and chloride (used as a conservative tracer) via ion chromatography. Adsorption  
 205 densities were calculated by numerically integrating breakthrough curves and dividing by  
 206 adsorbent mass (Equation S6).

207

## 208 **2.5 Continuous Regeneration Experiments**

209 Regeneration experiments were similar to adsorption experiments, except with 0.1 M H<sub>2</sub>SO<sub>4</sub>  
 210 pumped at 22.5 mL/min for 2 hours and samples collected every 10 minutes. Regeneration  
 211 efficiencies were calculated by dividing moles of ammonium eluted (integration of elution curve,  
 212 Figure S1) by the moles adsorbed (Equation S7).

213

## 214 **2.6 Modeling**

215 To account for non-ideality of concentrated ionic solutions, PHREEQC software<sup>33</sup> was used to  
 216 determine Pitzer activity coefficients based on the concentrations in each initial solution. Cation  
 217 chromatography measures total ammonia concentrations. Ammonia/ammonium speciation was  
 218 determined according to Equations 2-4 using measured values of pH and temperature:<sup>34</sup>

$$219 \quad K_{NH_4^+|T_2} = K_{NH_4^+|T_1} x \exp \left[ \frac{\Delta H_R}{R} \left( \frac{1}{T_1} - \frac{1}{T_2} \right) \right] \quad (2)$$

$$220 \quad [NH_4^+] = \frac{N_{tot}}{1 + \gamma_{NH_4^+} 10^{pH - pK_{NH_4^+}}} \quad (3)$$

$$221 \quad \{NH_4^+\} = \gamma_{NH_4^+} [NH_4^+] \quad (4)$$

222

223 where  $K_{NH_4^+}$  is the ammonium acid dissociation constant at 25 °C (9.25),<sup>30</sup> R is the universal gas  
224 constant, T is temperature,  $N_{TOT}$  is total ammonia concentration,  $[\ ]$  denotes molar concentration,  
225  $\{ \}$  denotes chemical activity, and  $\gamma_{NH_4^+}$  is the Pitzer activity coefficient for ammonia.

226

227 Adsorption curves were fit to the single-solute Langmuir model for each adsorbent (Equation 5,  
228 where  $n=1$ ).<sup>35</sup>  $q_f$  is the adsorption density (mmol  $NH_4^+$ ,  $Na^+$ , or  $K^+$ /g adsorbent),  $q_{max}$  is  
229 maximum adsorption density,  $K_{ads}$  is the affinity constant, and  $\{A\}$  denotes the chemical activity  
230 of species A. Although many previous studies have used linearization to determine maximum  
231 adsorption density and affinity constants, this approach can introduce statistical biases.<sup>36,37</sup> Thus,  
232 we used a non-linear regression to determine maximum adsorption density and affinity constants  
233 with ISOFIT (Isotherm Fitting Tool).<sup>38</sup>

234

235 For synthetic urine, experimental results were evaluated with three competitive adsorption  
236 models. The first was the competitive Langmuir model (Equation 5, where  $n=3$  for  $NH_4^+$ ,  $Na^+$ ,  
237 and  $K^+$ ).<sup>35</sup> The values of  $q_{max}$  and  $K_{ads}$  calculated from the single-cation adsorption experiments  
238 were used as inputs to the competitive Langmuir model, which was plotted for various activities  
239 using non-linear parameterization in MATLAB (8.3.0 R2014A). The second was a three-solute  
240 competitive adsorption model based on Jain and Snoeyink (Equation 6, see section S1.1 for more  
241 detail);  $q_{max}$  and  $K_{ads}$  for each cation were from single-cation adsorption experiments, and  
242 numerical subscripts denote each cation from lowest (1) to highest (3) maximum adsorption  
243 density.<sup>39</sup> The third was the empirical Langmuir-Freundlich model (Equation 7), in which  $K_{ads}$   
244 values were from single-solute experiments, and  $n$  and  $q_{max}$  (one value for all cations) were  
245 determined by nonlinear regression on synthetic urine data. For all three models, adsorption

246 densities were calculated using the experimentally measured equilibrium activities in synthetic  
 247 urine. To predict equilibrium adsorption densities and activities in undiluted real urine, we used  
 248 initial activities and model parameters to solve a system of six equations containing model  
 249 predictions for each cation and mass balances on each cation (section S1.1).

$$250 \quad q_{f,i} = \frac{K_{ads,i}q_{max,i}\{A_i\}}{1+\sum_{n=1} K_{ads,n}\{A_n\}} \quad (5)$$

$$251 \quad q_{f,3} = \frac{q_{max,1}K_{ads,3}\{A_3\}}{1+K_{ads,1}\{A_1\}+K_{ads,2}\{A_2\}+K_{ads,3}\{A_3\}} + \frac{(q_{max,2}-q_{max,1})K_{ads,3}\{A_3\}}{1+K_{ads,2}\{A_2\}+K_{ads,3}\{A_3\}} + \frac{(q_{max,3}-q_{max,2})K_{ads,3}\{A_3\}}{1+K_{ads,3}\{A_3\}} \quad (6)$$

$$252 \quad q_{f,i} = \frac{K_{ads,i}q_{max}\{A_i\}^n}{1+\sum_{n=1} K_{ads,n}\{A_i\}^n} \quad (7)$$

253  
 254 Material cost for different adsorbents was evaluated as an initial analysis of feasibility. Three  
 255 major determinants of adsorbent cost per gram nitrogen recovered ( $P_N$ ) were considered: specific  
 256 adsorbent price ( $P_{adsorbent}$ , in USD/kg resin), adsorption capacity ( $q_0$  in mmol N/g adsorbent), and  
 257 number of uses before adsorbent replacement ( $N$ ) (Equation 8, where  $MW_N$  is the molecular  
 258 weight of nitrogen). Adsorption capacities were the highest values measured in undiluted real  
 259 urine; resin prices were determined from literature (Table S5). Adsorbent cost per gram nitrogen  
 260 was also converted to cost per liter of urine treated ( $P_U$ ) by considering the total ammonia  
 261 concentration in urine in mg N/L ( $[NH_3]_{tot}=[NH_4^+] + [NH_3]$ , Equation 9).

$$262 \quad P_N = \frac{P_{adsorbent}}{Nq_0MW_N} \quad (8)$$

$$263 \quad P_U = P_N[NH_3]_{tot} \quad (9)$$

264 For each adsorbent tested, experimental adsorption density values were used to determine the  
 265 reactor volume (Equation 10).  $D_U$  is urine production rate per person (L urine/(person\*day)),  $P_H$   
 266 is average household size (people/household),  $t_c$  is time between collection,  $q$  is experimental  
 267 adsorption density (mg  $NH_4^+$ -N/g adsorbent), and  $\rho_b$  is bulk density (g adsorbent/L reactor

268 volume). We assumed that the ion exchange cartridge would be replaced weekly and treat 28  
269 liters of urine per week for a household with four people each producing one liter of urine each  
270 day. Bulk densities were determined by weighing known volumes of packed adsorbents.

$$271 \quad V_R = \frac{D_U * P_H * t_c * [NH_3]_{tot}}{q * \rho_b} \quad (10)$$

## 272 **2.7 Statistical Analysis**

273 Best-fit Langmuir parameters ( $q_{max}$  and  $K_{ads}$ ) determined from non-linear regression were  
274 compared for each pair of adsorbents with a one-way ANOVA and paired t-tests. A similar  
275 analysis was performed to compare solutions (pure salt, synthetic urine, and real urine). The  
276 single-solute Langmuir isotherm was applied to all solutions for consistency in the statistical  
277 analysis (Table S6). Although both  $q_{max}$  and  $K_{ads}$  were compared for each isotherm, only  $q_{max}$   
278 was reported because it was a more conservative indicator of significant differences and was  
279 more relevant to high ammonium concentrations in urine. Ammonium adsorption densities in  
280 experimental triplicates with undiluted real urine for each adsorbent were also compared with a  
281 one-way ANOVA and paired t-tests.

282

## 283 **3. RESULTS AND DISCUSSION**

### 284 **3.1 Comparison of Adsorbents at pH 4**

285 Based on experiments with  $NH_4Cl$  at pH 4, the four adsorbents exhibited different adsorption  
286 capacities (Figure 1a); however, the best-fit maximum adsorption densities were not statistically  
287 different ( $p > 0.05$ ). More variability was observed at high concentrations because of high  
288 dilution factors (e.g., 1:1000 for highest concentrations); they were accepted because of the  
289 redundancy present with sixteen points per adsorption curve. The Langmuir model was used  
290 because we expected a finite number of identical adsorption sites for zeolite and the synthetic

291 resins and previous studies reported it had the best fit for the adsorbents tested.<sup>15,23,26,40</sup> Best-fit  
292 maximum adsorption densities and affinity constants are summarized in Table S4 and Figure S2.  
293 A similar analysis was performed for NaCl and KCl to determine Langmuir parameters for later  
294 use in the competitive adsorption model (Figure S3).

295  
296 Overall, the adsorption capacities and affinity constants for pH 4  $\text{NH}_4\text{Cl}$  from this study were  
297 higher than those in literature (Table S1, Table S4).<sup>22,23,26,27,29</sup> For natural adsorbents, different  
298 sources (e.g. clinoptilolite from Turkey or USA)<sup>22</sup> and pretreatment (pyrolysis temperature and  
299 time)<sup>26</sup> could contribute to variation in best-fit Langmuir parameters between studies. For all  
300 adsorbents, variation could be due to operation at much higher concentrations that show more of  
301 the adsorption curve and the use of non-linear regression for fitting ( $q_{\text{max}}$  values determined by  
302 linearization of the Langmuir isotherm were lower; data not shown). Note that the estimate for  
303 the maximum ammonium adsorption capacity for Dowex Mac 3 was significantly higher than  
304 the highest value measured directly, which is one limitation of using best-fit parameters to  
305 compare isotherms.

306

### 307 **3.2 Effect of pH on Ammonium Adsorption**

308 Adsorption results for the pH 9  $\text{NH}_4\text{Cl}$  solutions are presented in Figure 1b. Although the  
309 adsorption densities were higher for the synthetic resins than the natural adsorbents, there were  
310 no statistically significant differences between adsorbents due to the high variability observed.  
311 Ammonium adsorption isotherms at pH 4 and pH 9 were also not significantly different for any  
312 adsorbent, but several observations can be made about the effects of pH on adsorption sites and  
313 ammonia speciation. Cation adsorption sites are most effective when negatively charged, which

314 occurs when solution pH exceeds the surface point of zero charge. This effect was especially  
315 apparent for Dowex Mac 3, which has a reported pK<sub>a</sub> of 5 (Table S1), which is between the two  
316 pH values tested for NH<sub>4</sub>Cl solutions. In the pH 4 solutions, substantially fewer sites were  
317 deprotonated than in the pH 9 solutions. Accordingly, fewer sites were available for ammonium  
318 adsorption and lower adsorption densities were observed, especially at low equilibrium activities.  
319 Similar trends have been reported for clinoptilolite.<sup>41</sup>

320

321 The solution pH also impacted NH<sub>4</sub><sup>+</sup> adsorption by affecting ammonia speciation. Given the  
322 proximity of the pH in pH 9 NH<sub>4</sub>Cl, synthetic urine, and real urine experiments to the NH<sub>3</sub>/ NH<sub>4</sub><sup>+</sup>  
323 pK<sub>a</sub> (9.25), up to 35% of total ammonia was present as NH<sub>3</sub>. Because NH<sub>3</sub> is uncharged and thus  
324 does not participate in cation exchange, we expected the adsorption density to be lower for the  
325 pH 9 solutions than the pH 4 solutions. Although this was the trend for the natural adsorbents, it  
326 was not the case for the synthetic resins. One possible reason for the difference is that natural  
327 adsorbents have more heterogeneous adsorption sites and initial adsorbates and therefore more  
328 complex pH effects (Figure S4).

329

330 In interpreting the pH results, it is important to note that the final pH of the solutions, after  
331 adsorption equilibrium was established, was different in some cases than the initial solution pH;  
332 the equilibrium pH values of the highest concentrations tested for each solution are shown in  
333 Figure S5. The equilibrium pH was affected by two competing phenomena. The first was  
334 sorption of NH<sub>4</sub><sup>+</sup>, which removes it from solution and shifts the NH<sub>3</sub>/ NH<sub>4</sub><sup>+</sup> equilibrium, causing  
335 protonation of some NH<sub>3</sub> and increasing solution pH. The second was desorption of protons due  
336 to exchange with other cations, which decreases solution pH. For the pH 4 solutions, the solution

337 pH decreased after equilibrating with the synthetic resins, indicating that desorption of protons  
338 was the dominant effect. With natural adsorbents exposed to pH 4 solutions, the pH increased,  
339 indicating that  $\text{NH}_3/\text{NH}_4^+$  equilibrium dominated. In addition, natural adsorbents were initially  
340 loaded with a mixture of protons and other cations, leading to relatively fewer  $\text{H}^+$  desorbing.  
341 Batch experiments with sulfuric acid confirmed this phenomenon, as  $\text{Na}^+$ ,  $\text{K}^+$ , and  $\text{Ca}^{2+}$  ions  
342 desorbed from natural adsorbents but not from synthetic resins (Figure S4). At pH 9, the  $\text{NH}_3/\text{NH}_4^+$   
343 pair buffered the pH and only small pH changes were observed (Figure S5). Synthetic  
344 urine and real urine pH values also increased (slightly) for natural adsorbents and decreased for  
345 synthetic resins (Figure S5).

346

### 347 **3.3 Effect of Competition on Ammonium Adsorption**

348 The effect of competition was investigated by performing adsorption experiments in synthetic  
349 urine, in which  $\text{Na}^+$  and  $\text{K}^+$  competed with  $\text{NH}_4^+$  for adsorption sites (Figure 2). Again, the  
350 synthetic resins adsorbed more ammonium per gram than the natural adsorbents. In particular,  
351 the maximum adsorption density ( $q_{\text{max}}$  from best-fit single-solute Langmuir isotherm) of Dowex  
352 Mac 3 was significantly higher than the other three adsorbents ( $p < 0.01$  with Dowex 50;  
353  $p < 0.0001$  with clinoptilolite and biochar). There was no significant difference between  
354 adsorption capacities for the pure  $\text{NH}_4\text{Cl}$  and synthetic urine solutions ( $p > 0.05$ ), indicating that  
355 the presence of other constituents, including competing ions, did not decrease the adsorption  
356 density of ammonium on any of the adsorbents.

357

358 Synthetic urine adsorption data were fitted to three models: competitive Langmuir, trisolute  
359 Jain/Snoeyink, and competitive Langmuir-Freundlich (Figure 2) and the average relative error



360 and sum of squared error (SSE) were determined. For clinoptilolite, Dowex 50, and Dowex Mac  
361 3, the Langmuir-Freundlich model had the lowest SSE and best overall fit to synthetic urine data  
362 (Table S7), although it overestimated adsorption for clinoptilolite and Dowex 3 at low  
363 equilibrium activities (Figure S6). It is not surprising that the Langmuir-Freundlich model was  
364 superior because the parameters  $q_{\max}$  and  $n$  (Equation 7) were determined by fitting to the  
365 synthetic urine data (using nonlinear regression), whereas the Jain-Snoeyink and competitive  
366 models were based exclusively on the  $q_{\max}$  and  $K_{\text{ads}}$  parameters determined from single-solute  
367 Langmuir fits. For biochar, competitive Langmuir was the best fit overall (Table S7), but it  
368 overestimated adsorption at low equilibrium activities (Figure S6). The Jain-Snoeyink model  
369 assumes competitive Langmuir behavior below the maximum adsorption densities of sodium and  
370 potassium and single-solute Langmuir for ammonium above those adsorption densities. There  
371 was not much difference between the competitive Langmuir and Jain-Snoeyink isotherms,  
372 primarily because single-solute  $q_{\max}$  values for  $\text{Na}^+$  and  $\text{NH}_4^+$  differed by at most 0.74 mmol N/g  
373 adsorbent (Dowex 50, Table S4).

374  
375 The fact that the competitive Langmuir model predicted lower adsorption densities in synthetic  
376 urine than were measured could be due to overestimating the impact of competitor cations or  
377 because other constituents in the synthetic urine increased adsorption (such as acetate; see  
378 section 3.5). Single solute ammonium adsorption densities, which isolate the former effect, were  
379 higher than competitive Langmuir models for clinoptilolite (38%), biochar (64%), Dowex 50  
380 (75%), and Dowex Mac 3 (18%). Larger differences between competitive and single-solute  
381 models may indicate less homogeneous sites and thus more selectivity for ammonium. Even if  
382 adsorption sites are identical, access to them may vary based on macroscopic pore size

383 distributions. Hydrated ionic radius is one proxy for access to adsorption sites;<sup>42</sup> ammonium and  
384 potassium ions have smaller radii than sodium ions,<sup>43</sup> allowing the former species to diffuse  
385 through smaller pores and access more exchange sites. However, the  $q_{\max}$  values for  $\text{NH}_4^+$  and  
386  $\text{Na}^+$  from single-solute experiments were similar (Table S4), suggesting that differences in  
387 hydrated ionic radius did not completely explain differential adsorption of cations.

388

### 389 **3.4 Adsorption in Real Urine**

390 The isotherm trends observed in synthetic urine adsorption were similar to those in real urine  
391 (Figure 3a, Dowex Mac 3 > Dowex 50 > clinoptilolite ~biochar). Maximum ammonium  
392 adsorption densities ( $q_{\max}$  from best-fit single-solute Langmuir isotherm) were significantly  
393 different for all adsorbent pairs except clinoptilolite and biochar. The Dowex Mac 3 adsorption  
394 isotherm had the highest maximum adsorption density ( $p < 0.001$  for pair-wise comparison with  
395 all other adsorbents). To provide a more direct comparison between the adsorbents for the  
396 specific case of real urine, and to overcome the variability observed in the isotherms, triplicate  
397 adsorption experiments were conducted with undiluted real urine (Figure 3b). Dowex Mac 3 had  
398 a statistically higher  $\text{NH}_4^+$  adsorption density than all other adsorbents ( $p < 0.001$  for clinoptilolite  
399 and biochar;  $p < 0.05$  for Dowex 50). Together, these results support the conclusion that Dowex  
400 Mac 3 exhibited a higher adsorption density than clinoptilolite, biochar, and Dowex 50. Given its  
401 manufactured nature, Dowex Mac 3 was expected to have a higher maximum adsorption density  
402 than the heterogeneous natural adsorbents; it was also expected to have a higher maximum  
403 adsorption density than Dowex 50 because of its aliphatic resin structure and macropores, which  
404 have more surface area available for adsorption than the polystyrene backbone of Dowex 50  
405 (Table S1).

406

407 The three competitive models from synthetic urine isotherms were also applied to adsorption in  
408 undiluted real urine (Table S8). The Jain-Snoeyink model was best for predicting adsorption  
409 densities in real urine. The main reason is because the adsorption density in real urine was lower  
410 than that measured in synthetic urine at similar equilibrium activity levels (even though the  
411 differences were not statistically significant; see next section). Thus, the Langmuir-Freundlich  
412 overestimated adsorption density in undiluted real urine.

413

414 To provide more insight into the differential adsorption of competitor cations (Figure 3b), the  
415 adsorption isotherms for  $\text{NH}_4^+$ ,  $\text{Na}^+$ , and  $\text{K}^+$  in real urine on Dowex Mac 3 are shown in Figure  
416 4a. As expected given its sixfold (relative to  $\text{Na}^+$ ) or tenfold (relative to  $\text{K}^+$ ) higher molar  
417 concentration in urine, ammonium occupied the majority of available sites. Preferential  
418 adsorption of  $\text{NH}_4^+$  was also observed, as seen by the higher adsorption density of ammonium  
419 compared to the other cations at the same equilibrium activity. Similar trends were observed for  
420 the other adsorbents, even though they are not reported to have higher affinities for ammonium.

421

422 To confirm that ion exchange was the primary sorption mechanism in real urine, the  
423 characteristic free energy of adsorption in undiluted real urine was determined using the  
424 Dubinin-Radushkevich isotherm. The free energy of adsorption for every adsorbent was in the  
425 ion exchange range ( $>8$  kJ/mol),<sup>36</sup> indicating that ion exchange was a more significant factor  
426 than van der Waals interactions (Figure S7).

427

428 **3.5 Comparison of Solutions**

429 For all adsorbents, there were no statistically significant differences between ammonium  
430 adsorption curves in different solutions (Figure 3b, Dowex Mac 3; all other resins, Figure S8,  
431  $p > 0.05$ ). Given the higher ionic strength in urine compared to  $\text{NH}_4\text{Cl}$ , we expected less  
432 adsorption in real and synthetic urine than the pure salt solutions due to charge screening.<sup>44</sup>  
433 However,  $\text{NH}_4^+$  adsorption densities in urine solutions were not significantly different than in  
434 pure salt solutions when plotted relative to both equilibrium concentration and equilibrium  
435 activity, which accounts for ionic strength differences (Figure S9,  $p > 0.05$ ). Charge screening can  
436 be complicated by several factors: the presence of macropores, because sites deep within  
437 macropores are less affected by solution characteristics; net surface charge and the distribution of  
438 charged surface moieties; and electrostatic effects of previously adsorbed molecules.<sup>45</sup>

439  
440 In addition to ionic strength, the presence of organics may also affect ammonium adsorption.  
441 Organics have been documented to lead to higher  $\text{NH}_4^+$  uptake by ion exchange materials due to  
442 a reduction in surface tension that increases access to macroporous sites.<sup>23</sup> In our experiments,  
443 synthetic urine contained only acetic acid whereas real urine is known to contain acetic acid as  
444 well as amino acids; organic acids have been shown to decrease the surface tension of water.<sup>46,47</sup>  
445 Jorgensen and Weatherley also determined that the enhancement of ammonium adsorption was  
446 not as large at higher adsorption densities,<sup>23</sup> which is the same trend observed when comparing  
447 synthetic and real urine with pure salt solutions. Thus, organic compounds present in synthetic  
448 and real urine but absent in pure salt solutions may enhance adsorption density for macroporous  
449 sites. Real and synthetic urine adsorption curves were not significantly different ( $p > 0.05$ ),  
450 indicating that synthetic urine was a sufficient proxy and that the more heterogeneous mixture of  
451 organics in real urine did not significantly affect ammonium adsorption.

452

### 453 **3.6 Continuous Flow Adsorption**

454 While batch experiments were useful for characterizing adsorption isotherms, nutrient recovery  
455 from urine using ion exchange would most likely be implemented in continuous-flow column  
456 configuration. To complement the batch data, breakthrough curves in continuous-flow columns  
457 were generated to compare adsorbents (Figure 5a). In control columns with no resin,  $\text{NH}_4^+$  and  
458  $\text{Cl}^-$  mass balances were within 5% (Figure S10). Calculated adsorption densities were 1.91 mmol  
459 N/g for biochar, 2.00 for clinoptilolite, 2.74 for Dowex 50, and 4.23 for Dowex Mac 3.  
460 These results are similar to batch results (e.g., Fig 3b), confirming that Dowex Mac 3 had the  
461 highest adsorption capacity. Importantly, the ammonia concentrations measured during column  
462 experiments were less variable than those measured during batch experiments. Possible reasons  
463 include the use of lower dilution factors (e.g., note that less variability is observed for the lowest  
464 concentrations, similar to the batch experiments) and the potential for more ammonia  
465 volatilization to occur during the 24-h batch tests.

466

### 467 **3.7 Regeneration**

468 Column regeneration was performed for one cycle as a proof-of-concept and regeneration  
469 efficiencies were calculated for each adsorbent. The synthetic resins both showed almost 100%  
470 regeneration (Dowex 50 95%, Dowex Mac 3 99%). Clinoptilolite had a regeneration efficiency  
471 of 43%, indicating that not all ammonium was eluted; biochar had a regeneration over 100%,  
472 indicating elution of initially loaded ammonium or biochar decomposition. These natural  
473 adsorbents may still be promising for direct application as a solid fertilizer.<sup>48,49</sup>

474

### 475 3.8 Feasibility Assessment

476 As an initial assessment of feasibility, adsorbent cost was determined for recovering nitrogen by  
477 ion exchange according to Equation 8. Material cost for each adsorbent was determined from  
478 literature values and the adsorption densities were those determined from the triplicate batch  
479 experiments in undiluted real urine (Table S5). Based on the low recovery of ammonium from  
480 clinoptilolite, it would likely only be used once; however, better regeneration may be possible  
481 with other regenerants or other conditions. Thus, for comparison with synthetic resins, we show  
482 adsorbent costs for a single use up to 100 uses assuming 100% regeneration efficiency (Figure  
483 5).

484  
485 For a single use, clinoptilolite had the lowest adsorbent cost/g N because of its low material cost,  
486 even though its adsorption capacity is lower than the synthetic resins. However, a more  
487 expensive adsorbent can result in a lower treatment cost if it is more regenerable. For example, if  
488 clinoptilolite is used once, treatment would cost \$7.40/kg N; if Dowex Mac 3 is used 100 times,  
489 treatment would cost \$6.00/kg N.

490  
491 Adsorbent costs (\$/g N) were compared to the cost of conventional nitrogen removal (Figure 5b,  
492 dotted line).<sup>50</sup> We are currently investigating other regenerants (e.g., HCl, HNO<sub>3</sub>) over many  
493 regeneration cycles to more conclusively evaluate long-term regeneration potential and costs.  
494 With 100% regeneration efficiency, material costs are at or below the cost of biological nitrogen  
495 removal if Dowex Mac 3 is used as few as ten times; the natural adsorbents used only once still  
496 have a lower material cost than conventional nitrogen removal. In addition, we expect nitrogen  
497 recovery to have additional benefits compared to removal, including revenue generated from

498 value-added products like fertilizer. The same data in Figure 5b can also be calculated per liter of  
499 urine using Equation 9 (Figure S11).

500

501 Reactor volume will also impact process costs and feasibility. To treat the urine produced by a  
502 family of four over one week, the reactor volume required for Dowex Mac 3 was the lowest (5.3  
503 L), followed by Dowex 50 (5.8 L), clinoptilolite (8.9 L), and biochar (19 L)(Figure S12).

504 Biochar required a much larger reactor volume because of its markedly lower bulk density  
505 (Table S5).

506

507 This analysis illustrates that the adsorbent costs and reactor volumes may be feasible and that  
508 further analysis of the potential for ion exchange adsorbents is warranted. Multicomponent  
509 models like the Jain-Snoeyink can help predict adsorption capacities based on influent urine  
510 concentrations, which can vary (Figure S13). Many other factors besides regeneration potential  
511 and adsorption density will affect the cost of recovering nitrogen via ion exchange, including  
512 other materials for producing cartridges and regeneration facilities, whether the adsorbents are  
513 installed at individual toilets or at the building scale, the cost of regenerant, transport distances,  
514 and the final fertilizer product quality and market value. Because the other factors are relatively  
515 independent of adsorbent material, however, the simple analysis presented here is useful for  
516 comparing adsorbents used in the same configuration, which was the overall objective of this  
517 investigation.

518

519 **3.9 Potential Implications for Urine Treatment**

520 Characterization of four different ion exchange adsorbents has provided a proof-of-concept for  
521 nitrogen recovery from source-separated urine via ion exchange. Once their adsorption capacity  
522 is reached, natural adsorbents like clinoptilolite and biochar could be applied directly as  
523 fertilizer, assuming pathogen concerns can be addressed. Alternatively, ammonium concentrate  
524 could be produced by eluting ammonium from any adsorbent. The process modeling conducted  
525 in this study can also be used to specify adsorption capacities and regeneration lifetimes required  
526 for newly developed adsorbents to be cost effective for nitrogen recovery from urine.

527

528 Several process engineering questions are recommended for future research, including  
529 optimizing elution of the ammonium to produce a concentrated solution that can feed into  
530 fertilizer or other products, and how to combine ion exchange with other nutrient recovery  
531 processes, like struvite precipitation. These questions are best investigated using column  
532 operation. Additional post-treatment, such as pharmaceutical removal from the eluent or eluate,  
533 or converting liquid fertilizer to solid, may be desirable and will affect process costs.

534

535 Ion exchange adsorbents could be employed in on-site or centralized wastewater treatment. A  
536 decentralized scheme might involve a service provider that regularly collects and replaces  
537 household cartridges and transports them to a centralized regeneration facility. Alternatively,  
538 cation exchange adsorbents could be used and regenerated on-site at a central facility at which  
539 source-separated urine is collected (by manual transport, such as high-density slums, or via  
540 dedicated pipes in a large building). Other implementation factors to consider include variability  
541 in urine composition, location of treatment facilities, method and cost of transport, and degree of



542 centralization. For example, lifecycle impacts and costs have recently been modeled for  
543 phosphate recovery and trace organic removal via ion exchange.<sup>51</sup>

544  
545 Because source separation has not yet been widely adopted, resource recovery technologies like  
546 ion exchange can potentially influence the design and scale of source separation systems. In this  
547 study we have demonstrated that ammonium can be recovered from urine using ion exchange  
548 and compared the efficacy of natural and synthetic adsorbents. Further work on continuous-flow  
549 recovery, optimal scale, and integration with other processes will add to the base of knowledge  
550 for potential application of novel technologies for nitrogen recovery from source-separated urine.  
551 Another promising direction for future research is the recovery of ammonium from other high-  
552 strength wastes, such as digestate and agricultural waste streams.

553

#### 554 **ASSOCIATED CONTENT**

555 The Supporting Information (SI) contains single solute adsorption curves, details on isotherm  
556 modeling, and calculations and results for financial feasibility. This information is available free  
557 of charge via the Internet at <http://pubs.acs.org>.

558

#### 559 **AUTHOR INFORMATION**

560 Corresponding author (K.L.N.):

561 Phone: 510-643-5023; fax: 510-642-7483; e-mail: [karanelson@berkeley.edu](mailto:karanelson@berkeley.edu)

#### 562 **Notes**

563 The authors declare no competing financial interests.

564

565 **ACKNOWLEDGEMENTS**

566 W.A.T. and K.L.N. acknowledge research funding from the National Science Foundation (NSF)  
567 through the ReNUWIt Engineering Research Center (<http://renuwit.org>; NSF Grant No. CBET-  
568 0853512). W.A.T. was also supported by an NSF Graduate Research Fellowship (NSF Grant No.  
569 DGE 1106400) and a Ford Foundation Fellowship. Much of this work was conducted on a  
570 research exchange at Eawag during which K.M.U. was a gracious host. We acknowledge Karin  
571 Rottermann and Claudia Bänninger-Werffelli for their excellent assistance with cation analysis  
572 and Maritza Flores-Marquez for her work on preliminary isotherms.

573 **References**

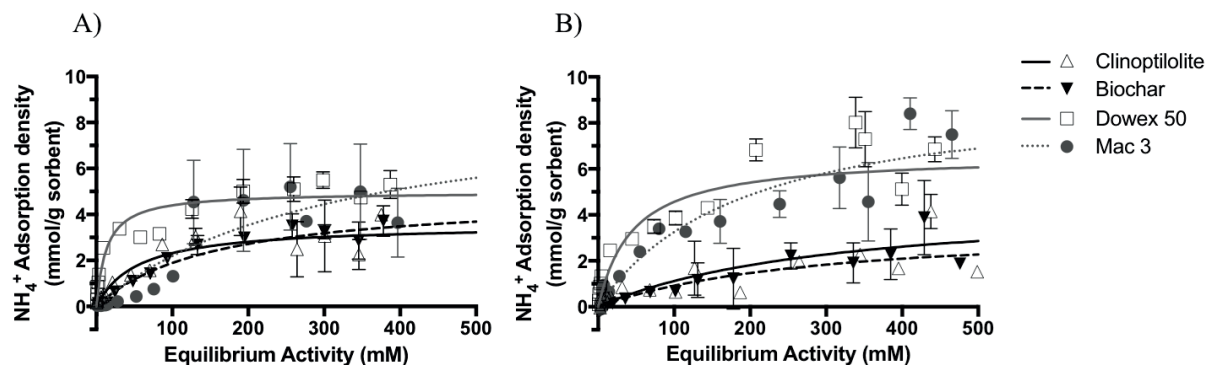
- 574 (1) *Source Separation and Decentralization for Wastewater Management*, 1st ed.; Larsen, T. A.,  
575 Udert, K. M., Lienert, J., Eds.; IWA Publishing, 2013.
- 576 (2) Ma, X. (Cissy); Xue, X.; González-Mejía, A.; Garland, J.; Cashdollar, J. Sustainable Water  
577 Systems for the City of Tomorrow—A Conceptual Framework. *Sustainability* **2015**, *7* (9),  
578 12071–12105.
- 579 (3) Tervahauta, T.; Hoang, T.; Hernández, L.; Zeeman, G.; Buisman, C. Prospects of Source-  
580 Separation-Based Sanitation Concepts: A Model-Based Study. *Water* **2013**, *5* (3), 1006–  
581 1035.
- 582 (4) Wood, A.; Blackhurst, M.; Hawkins, T.; Xue, X.; Ashbolt, N.; Garland, J. Cost-effectiveness  
583 of nitrogen mitigation by alternative household wastewater management technologies. *J.*  
584 *Environ. Manage.* **2015**, *150*, 344–354.
- 585 (5) Galloway, J. N.; Dentener, F. J.; Capone, D. G.; Boyer, E. W.; Howarth, R. W.; Seitzinger,  
586 S. P.; Asner, G. P.; Cleveland, C. C.; Green, P. A.; Holland, E. A.; et al. Nitrogen Cycles:  
587 Past, Present, and Future. *Biogeochemistry* **2004**, *70* (2), 153–226.
- 588 (6) Nordin, A.; Nyberg, K.; Vinnerås, B. Inactivation of *Ascaris* Eggs in Source-Separated Urine  
589 and Feces by Ammonia at Ambient Temperatures. *Appl. Environ. Microbiol.* **2009**, *75* (3),  
590 662–667.
- 591 (7) Fumasoli, A.; Etter, B.; Sterkele, B.; Morgenroth, E.; Udert, K. M. Operating a pilot-scale  
592 nitrification/distillation plant for complete nutrient recovery from urine. *Water Sci.*  
593 *Technol.* **2016**, *73* (1), 215–222.
- 594 (8) Jimenez, J.; Bott, C.; Love, N.; Bratby, J. Source Separation of Urine as an Alternative  
595 Solution to Nutrient Management in Biological Nutrient Removal Treatment Plants. *Water*  
596 *Environ. Res.* **2015**, *87* (12), 2120–2129.
- 597 (9) *The Pulse of the Bay: The State of Bay Water Quality, 2015 and 2065*; SFEI Contribution  
598 #759; San Francisco Estuary Institute: Richmond, CA, 2015.
- 599 (10) Aissa-Grouz, N.; Garnier, J.; Billen, G.; Mercier, B.; Martinez, A. The response of river  
600 nitrification to changes in wastewater treatment (The case of the lower Seine River  
601 downstream from Paris). *Ann. Limnol. - Int. J. Limnol.* **2015**, *51* (4), 351–364.
- 602 (11) Harris-Lovett, Sasha. *Water Infrastructure in the Face of Uncertainty: An Integrative*  
603 *Approach to Nitrogen Management in the San Francisco Bay Estuary*. Masters of Science,  
604 University of California at Berkeley, 2013.
- 605 (12) O’Keefe, M.; Lüthi, C.; Tumwebaze, I. K.; Tobias, R. Opportunities and limits to market-  
606 driven sanitation services: evidence from urban informal settlements in East Africa.  
607 *Environ. Urban.* **2015**, *27* (2), 421–440.
- 608 (13) Etter, B.; Udert, K. M.; Gounden, T. *Valorisation of Urine Nutrients (VUNA) Final*  
609 *Report*; Swiss Federal Institute of Aquatic Science and Technology (Eawag): Dübendorf,  
610 Switzerland, 2015.
- 611 (14) Udert, K. M.; Larsen, T. A.; Biebow, M.; Gujer, W. Urea hydrolysis and precipitation  
612 dynamics in a urine-collecting system. *Water Res.* **2003**, *37* (11), 2571–2582.
- 613 (15) Karadag, D.; Koc, Y.; Turan, M.; Armagan, B. Removal of ammonium ion from aqueous  
614 solution using natural Turkish clinoptilolite. *J. Hazard. Mater.* **2006**, *136* (3), 604–609.
- 615 (16) Beler-Baykal, B.; Cinar-Engin, S. Ion exchange with clinoptilolite to control ammonium  
616 in drinking water. *J. Water Supply Res. Technol.* **2007**, *56* (8), 541.

- 617 (17) Karadag, D.; Tok, S.; Akgul, E.; Turan, M.; Ozturk, M.; Demir, A. Ammonium removal  
618 from sanitary landfill leachate using natural Gordes clinoptilolite. *J. Hazard. Mater.* **2008**,  
619 *153* (1–2), 60–66.
- 620 (18) Beler Baykal, B.; Kocaturk, N. P.; Allar, A. D.; Sari, B. The effect of initial loading on the  
621 removal of ammonium and potassium from source-separated human urine via  
622 clinoptilolite. *Water Sci. Technol.* **2009**, *60* (10), 2515.
- 623 (19) O’Neal, J. A.; Boyer, T. H. Phosphate recovery using hybrid anion exchange: Applications  
624 to source-separated urine and combined wastewater streams. *Water Res.* **2013**, *47* (14),  
625 5003–5017.
- 626 (20) Landry, K. A.; Boyer, T. H. Diclofenac removal in urine using strong-base anion exchange  
627 polymer resins. *Water Res.* **2013**, *47* (17), 6432–6444.
- 628 (21) Boyer, T. H.; Landry, K.; Sendrowski, A.; O’Neal, J. Nutrient Recovery from Urine using  
629 Selective Ion Exchange. *Proc. Water Environ. Fed.* **2012**, *2012* (15), 1942–1943.
- 630 (22) Wang, S.; Peng, Y. Natural zeolites as effective adsorbents in water and wastewater  
631 treatment. *Chem. Eng. J.* **2010**, *156* (1), 11–24.
- 632 (23) Jorgensen, T. ; Weatherley, L. . Ammonia removal from wastewater by ion exchange in  
633 the presence of organic contaminants. *Water Res.* **2003**, *37* (8), 1723–1728.
- 634 (24) Beler-Baykal, B.; Allar, A. D.; Bayram, S. Nitrogen recovery from source-separated  
635 human urine using clinoptilolite and preliminary results of its use as fertilizer. *Water Sci.*  
636 *Technol. J. Int. Assoc. Water Pollut. Res.* **2011**, *63* (4), 811–817.
- 637 (25) Ding, Y.; Liu, Y.-X.; Wu, W.-X.; Shi, D.-Z.; Yang, M.; Zhong, Z.-K. Evaluation of  
638 Biochar Effects on Nitrogen Retention and Leaching in Multi-Layered Soil Columns.  
639 *Water. Air. Soil Pollut.* **2010**, *213* (1–4), 47–55.
- 640 (26) Kizito, S.; Wu, S.; Kipkemoi Kirui, W.; Lei, M.; Lu, Q.; Bah, H.; Dong, R. Evaluation of  
641 slow pyrolyzed wood and rice husks biochar for adsorption of ammonium nitrogen from  
642 piggery manure anaerobic digestate slurry. *Sci. Total Environ.* **2015**, *505*, 102–112.
- 643 (27) *DOWEX MAC-3 Engineering Information*; 177-01560–703; Dow Chemical Company,  
644 Dow Liquid Separations: Midland, MI, 2003.
- 645 (28) Lehmann, J.; Joseph, S. *Biochar for Environmental Management: Science and*  
646 *Technology*; Routledge, 2012.
- 647 (29) *DOWEX Fine Mesh Spherical Ion Exchange Resins For Fine Chemical and*  
648 *Pharmaceutical Column Separations*; 177-01509–904; Dow Chemical Company, Dow  
649 Water Solutions: Midland, MI.
- 650 (30) Perrin, D.D. *Ionization Constants of Inorganic Acids and Bases in Aqueous Solution*,  
651 *Second Edition*; Pergamon: Oxford, 1982.
- 652 (31) Udert, K.; Larsen, T.; Gujer, W. Fate of major compounds in source-separated urine.  
653 *Water Sci. Technol.* **2006**, *54* (11–12), 413–420.
- 654 (32) Udert, K. M.; Larsen, T. A.; Biebow, M.; Gujer, W. Urea hydrolysis and precipitation  
655 dynamics in a urine-collecting system. *Water Res.* **2003**, *37* (11), 2571–2582.
- 656 (33) Parkhurst, D. L.; Appelo, C. A. J. Description of input and examples for PHREEQC  
657 version 3—A computer program for speciation, batch-reaction, one-dimensional transport,  
658 and inverse geochemical calculations. In *U.S. Geological Survey Techniques and Methods*,  
659 *book 6*; 2013; Vol. 6, p 497.
- 660 (34) Pecson, B. M.; Nelson, K. L. Inactivation of *Ascaris suum* eggs by ammonia. *Environ. Sci.*  
661 *Technol.* **2005**, *39* (20), 7909–7914.

- 662 (35) *Water Quality Engineering: Physical / Chemical Treatment Processes*, 1 edition.; Wiley:  
663 Hoboken, N.J, 2013.
- 664 (36) Foo, K. Y.; Hameed, B. H. Insights into the modeling of adsorption isotherm systems.  
665 *Chem. Eng. J.* **2010**, *156* (1), 2–10.
- 666 (37) Dochain, D.; Vanrolleghem, P. *Dynamical Modelling and Estimation in Wastewater*  
667 *Treatment Processes*; IWA Publishing, 2001.
- 668 (38) Matott, L. S.; Rabideau, A. J. ISOFIT – A program for fitting sorption isotherms to  
669 experimental data. *Environ. Model. Softw.* **2008**, *23* (5), 670–676.
- 670 (39) Jain, J. S.; Snoeyink, V. L. Adsorption from Bisolute Systems on Active Carbon. *J. Water*  
671 *Pollut. Control Fed.* **1973**, *45* (12), 2463–2479.
- 672 (40) Xiong, C.; Han, X.; Yao, C. Sorption Behavior of In(III) Ions onto Cation-Exchange  
673 Carboxylic Resin in Aqueous Solutions: Batch and Column Studies. *Sep. Sci. Technol.*  
674 **2010**, *45* (16), 2368–2375.
- 675 (41) Kithome, M.; Paul, J. W.; Lavkulich, L. M.; Bomke, A. A. Effect of pH on ammonium  
676 adsorption by natural Zeolite clinoptilolite. *Commun. Soil Sci. Plant Anal.* **1999**, *30* (9–  
677 10), 1417–1430.
- 678 (42) Tobin, J. M.; Cooper, D. G.; Neufeld, R. J. Uptake of Metal Ions by *Rhizopus arrhizus*  
679 Biomass. *Appl. Environ. Microbiol.* **1984**, *47* (4), 821–824.
- 680 (43) Nightingale, E. R. Phenomenological Theory of Ion Solvation. Effective Radii of  
681 Hydrated Ions. *J. Phys. Chem.* **1959**, *63* (9), 1381–1387.
- 682 (44) Naidu, R.; Bolan, N. s.; Kookana, R. S.; Tiller, K. g. Ionic-strength and pH effects on the  
683 sorption of cadmium and the surface charge of soils. *Eur. J. Soil Sci.* **1994**, *45* (4), 419–  
684 429.
- 685 (45) Doula, M. K.; Ioannou, A. The effect of electrolyte anion on Cu adsorption–desorption by  
686 clinoptilolite. *Microporous Mesoporous Mater.* **2003**, *58* (2), 115–130.
- 687 (46) Bull, H. B.; Breese, K. Surface tension of amino acid solutions: A hydrophobicity scale of  
688 the amino acid residues. *Arch. Biochem. Biophys.* **1974**, *161* (2), 665–670.
- 689 (47) Álvarez, E.; Vázquez, G.; Sánchez-Vilas, M.; Sanjurjo, B.; Navaza, J. M. Surface Tension  
690 of Organic Acids + Water Binary Mixtures from 20 °C to 50 °C. *J. Chem. Eng. Data*  
691 **1997**, *42* (5), 957–960.
- 692 (48) Allar, A. D.; Baykal, B. B. An investigation into the potential use of nutrients recovered  
693 from urine diversion on a summer housing site: self-sufficiency based on nitrogen balance.  
694 *Water Sci. Technol.* **2016**, *73* (3), 576–581.
- 695 (49) Güereña, D.; Lehmann, J.; Hanley, K.; Enders, A.; Hyland, C.; Riha, S. Nitrogen  
696 dynamics following field application of biochar in a temperate North American maize-  
697 based production system. *Plant Soil* **2012**, *365* (1–2), 239–254.
- 698 (50) Falk, M. W.; Reardon, D. J.; Neethling, J. B.; Clark, D. L.; Pramanik, A. Striking the  
699 Balance between Nutrient Removal, Greenhouse Gas Emissions, Receiving Water  
700 Quality, and Costs. *Water Environ. Res.* **2013**, *85* (12), 2307–2316.
- 701 (51) Landry, K. A.; Boyer, T. H. Life cycle assessment and costing of urine source separation:  
702 Focus on nonsteroidal anti-inflammatory drug removal. *Water Res.* **2016**, *105*, 487–495.  
703

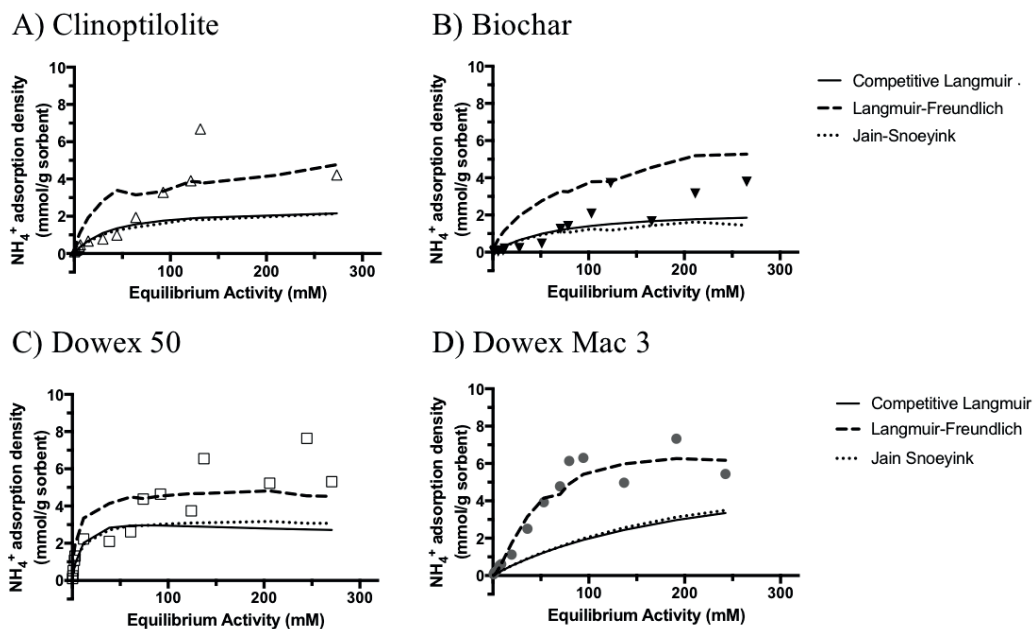
704

## 705 FIGURES

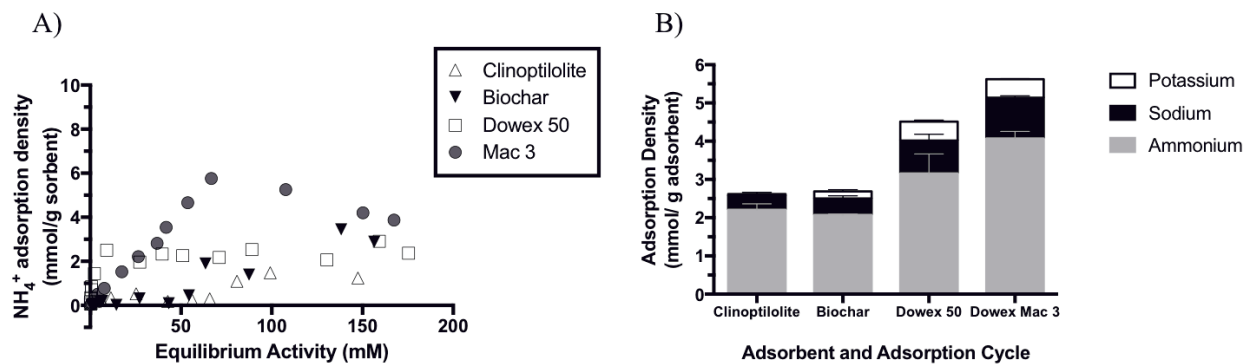


706  
707 **Figure 1.**  $\text{NH}_4^+$  adsorption in  $\text{NH}_4\text{Cl}$  (a) without pH adjustment and (b) for pH 9 solutions. Error  
708 bars represent one standard deviation above and below mean of dilution triplicates ( $n=3$ ) for high  
709 activities ( $> 100$  mM). Curves show best-fit Langmuir isotherms based on non-linear regression  
710 of experimental data.

711



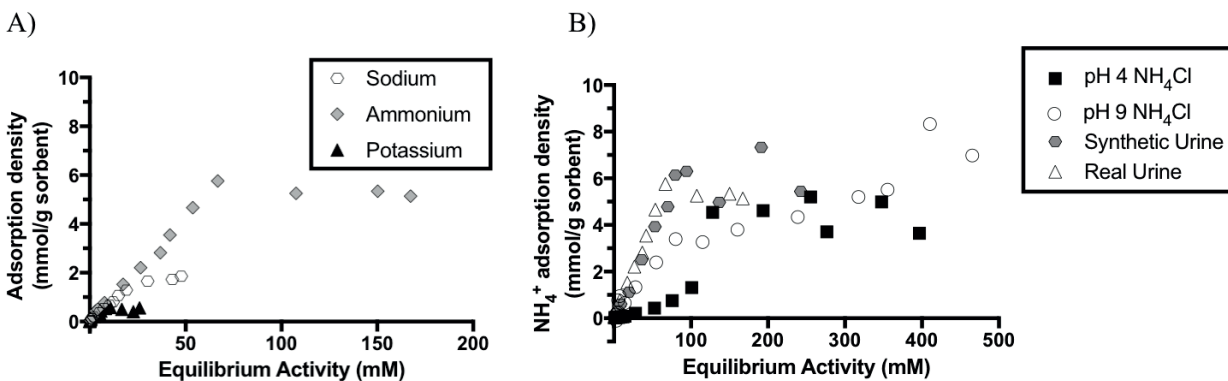
712  
713 **Figure 2.** Comparison of  $\text{NH}_4^+$  adsorption in synthetic urine and competitive Langmuir,  
714 competitive Langmuir-Freundlich, and Jain-Snoeyink models for (a) clinoptilolite, (b) biochar,  
715 (c) Dowex 50, and (d) Dowex Mac 3. Insets of lower equilibrium activities are in Figure S6.



716

717 **Figure 3.** (a)  $\text{NH}_4^+$  adsorption isotherm for real urine. (b) Adsorption density of  $\text{NH}_4^+$ ,  $\text{Na}^+$ , and  
 718  $\text{K}^+$  in undiluted real urine. Error bars represent one standard deviation above and below mean for  
 719 experimental triplicates ( $n=3$ ), and in some cases are too small to be shown.

720

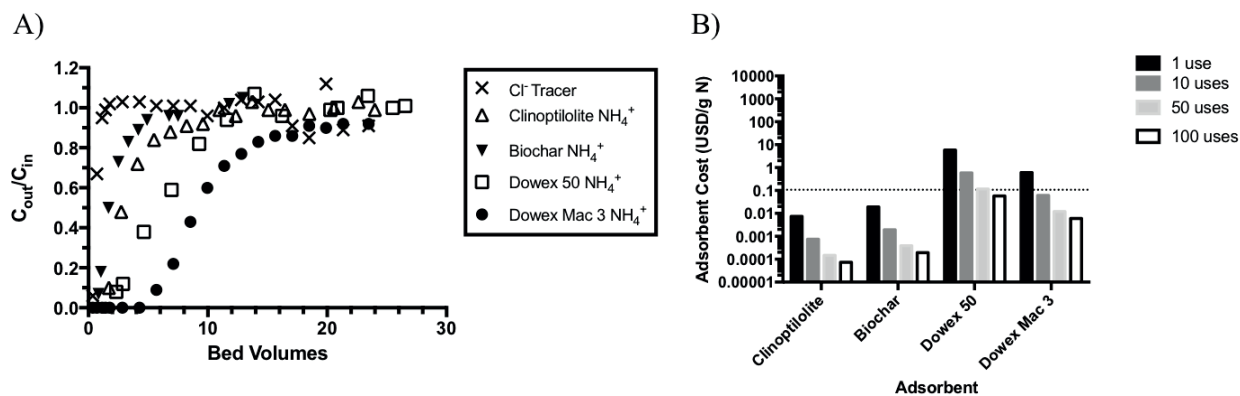


721

722 **Figure 4.** (a) Dowex Mac 3  $\text{NH}_4^+$ ,  $\text{Na}^+$ , and  $\text{K}^+$  adsorption in real urine. (b) Dowex Mac 3  $\text{NH}_4^+$   
 723 adsorption for all solutions.

724

725



726

727 **Figure 5.** (a) Adsorption breakthrough curves in continuous-flow columns. (b) Comparison of728 adsorbent cost for all four resins (in USD/g N) assuming 100% regeneration ( $r=1$ ). The dotted

729 line is the cost of conventional biological nitrogen removal per gram nitrogen removed

730 (horizontal line).<sup>50</sup>